Automatic Time-Dependent Coronal Hole Maps using Synchronized Multi-instrument EUV Data

Predictive Science Inc.

Ronald M. Caplan, Cooper Downs, and Jon A. Linker

Predictive Science Inc. 9990 Mesa Rim Road San Diego, CA 92121 www.predsci.com

AGU FALL MEETING

San Francisco | 15–19 December 2014

INTRODUCTION

Coronal holes (CHs) are manifested as relatively low intensity regions of the corona seen in EUV and X-Ray images and are usually associated with open magnetic field regions. Observing their evolution can help us understand how the Sun's magnetic field evolves in time and how these changes propagate out into the heliosphere. Estimations of the boundary of the CHs for a given image can be obtained manually without too much difficulty, however for time-dependent evolution, an automated approach is required. Additionally, the use of multiple instruments is needed to form synchronic maps with as much coverage as possible.

Here we display our recent attempts to automatically detect coronal holes using combined STEREO-A&B/EUVI-195A (STA,STB), and SDO/AIA-193A (AIA) imaging data.

To illustrate the method, we show the data-processing pipeline in steps for observations taken on 02/03/2011, which result in the CH map and EUV combined image displayed in the center of the poster. Time-sequences of coronal holes are also shown.

SUMMARY & FUTURE WORK

We have described a method of obtaining automatically generated coronal hole maps from STEREO-A/EUVI-195A, STEREO-B/EUVI-195A, and SDO/AIA-193A data. Our method relies on several often-overlooked pre-processing steps, and a custom region growing segmentation algorithm.

Two relevant additional data products of our investigation are the computation of inter-instrument scaling factors and limb brightening correction curves for each instrument over a four-year period, both of which can be obtained upon request.

Future work will involve improvements to the region growing algorithm to try to eliminate as much parameterization as possible, as well as adding time-dependent CH analysis tools.

This research is supported by funding from:

CH TIME EVOLUTION

The automated nature of the presented algorithm allows us to observe the evolution of CHs over time. An example of such evolution at 6-hour cadence from 01/30/2011 12:00 to 02/03/2011 18:00 is displayed below.

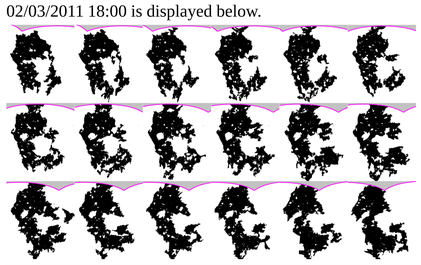

CH DETECTION ALGORITHM

The detection of CHs in EUV images is inherently an image segmentation problem. There are many methods for image segmentation, the simplest of which is intensity thresholding. which, for CH detection, is problematic due to overlap in intensity with dark filament channels and dark regions of the quiet sun.

Our method is a simplified region growing algorithm using one threshold (*t1*) for the seed placement and a second value (*t2*) for the stopping criteria. Since only local information is used, the region average and history do not need to be tracked and there is no order dependence. This allows the algorithm to be formulated in an embarrassingly parallel manner, which we have implemented in both FORTRAN-OpenMP and CUDA-C which are linked to MATLAB through MEX interface codes. (The GPU codes perform ~10X faster than the OpenMP on the test system). Additionally, we modify the standard 8-neighbor connectivity condition to require *n* consecutive marked pixels for inclusion in the region instead of one. The use of region growing avoids false detection of disconnected dark areas of quiet sun, while the modification of the consecutive pixel requirement helps to avoid false connectivity due to noise.

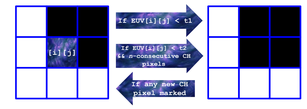

The algorithm starts with a blank CH map with pixel locations corresponding to missing/unused EUV data flagged. Each viable pixel location is independently checked to see if the EUV image at that location is below *t1*, and if it is, the pixel in the CH map is marked. Then, in each subsequent iteration, each pixel location is checked and if it is above *t1* and below *t2* and has at least *n* consecutive neighboring CH pixels, it is marked as a CH pixel. This iterative procedure continues until no additional points are added to the CH map.

The algorithm is applied to each instrument's EUV line-of-sight disk image, and then each one is mapped to a sin(theta)-phi plane with an inclusive overlap (since one perspective may see a CH which is obscured in another). We also produce a merged EUV image taking the minimum intensity value of overlaps to be able to judge the quality of the CH detection.

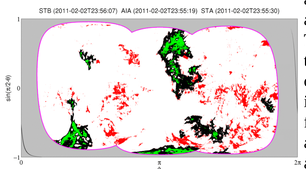

The image to the left shows the advantage of using a region growing approach versus standard thresholding. The green areas are the result of using a threshold of *t1*, the red areas of using only *t2*, and the black areas (which include green areas) the region resulting from our algorithm. We see that the algorithm captures the CH boundaries but avoids the large amount of dark quiet sun that is detected when using only *t2*.

The main challenge in using the algorithm is in choosing *t1* and *t2* such that a desired CH map is produced over large number of sequential frames. It is not clear if/how the CH intensities vary over the solar cycle (in which case the thresholds need to be modified over time), and the choice of *t2* is somewhat subjective (indeed the use of different colormaps in the EUV image can change the perceived detection quality). Future improvements to the algorithm are planned including additional stopping criteria (such as gradient values) to limit the sensitivity of *t2*, and ways of automatically choosing *t1*. Experimentation using the SRG algorithm of [Patt. Rec. Let. 26 (2005) 1139-1156] is also a possibility.

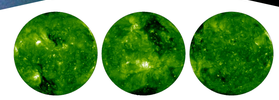

DATA ACQUISITION/PROCESSING

To obtain the EUV images, we have developed a set of custom IDL scripts which makes use of the well-known IDL script package SolarSoftWare (SSW). Time-synchronized images are found and undergo standard processing steps which includes exposure time correction and image registration, as well as unit conversion and bias, and flat field correction for EUVI data. The AIA images are binned to match the EUVI resolution and corrupted or obscured data is tested for and marked in order to exclude them from our processing algorithms.

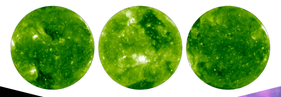

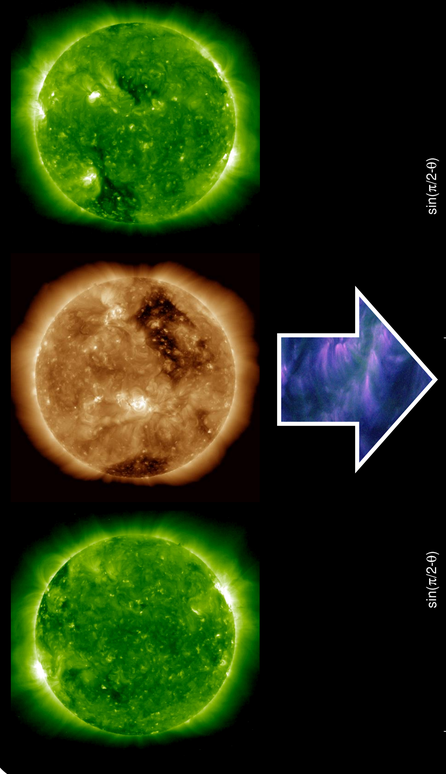

PSF DECONVOLUTION

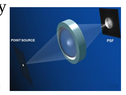

Optical effects such as scattered light, diffraction, and others modify the resulting images in ways which can cause many coronal hole detection algorithms to be less effective. Unwanted scattering of light can decrease the relative intensity contrast between CHs and nearby regions of the quiet sun, and cause CHs to be less uniformly dark.

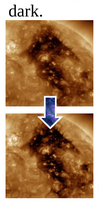

Point-spread functions (PSF) for both EUVI and AIA data are available which can be used to correct many of the effects.

We deconvolve the images using the PSFs which noticeably improves their quality. The deconvolution is performed using the GPU-accelerated software SGP-GPU [**M. Prato et al, A&A 539 (2012) A133**], which implements the SGP deconvolution algorithm [**S. Bonettini et al, Inv Prob 25 (1) (2009) 015002**] in C and CUDA. The use of the GPU code reduces the processing time for our set of images from weeks to hours.

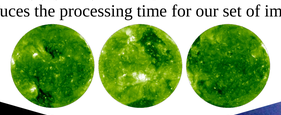

INTER-INSTRUMENT INTENSITY SCALING

DATA PRODUCT

In order to simplify the determination of intensity level thresholds in our detection algorithm, we scale images from the various instruments to each other. We take a data-driven approach and have produced MATLAB codes which compute a running average histogram of intensity data for each instrument, and then align the left-sides (since our focus is coronal holes) of the histograms of STB and AIA to that of STA using a minimum least-squares optimization utilizing a custom linesearch algorithm. To ensure that all three instruments view the same structures over the average window, we shift the data window for STB and AIA to match the start/stop central meridian angles of the STA time window. We have computed the scaling factors for STB->STA and AIA->STA from 2011 to 2014 using an average window of one year at a six-hour cadence which allows the use of the scale factors for any time-window of interest. We see that the scale factors change over time, reinforcing the need for a data driven approach.

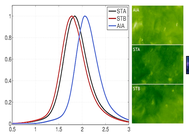

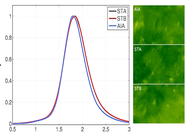

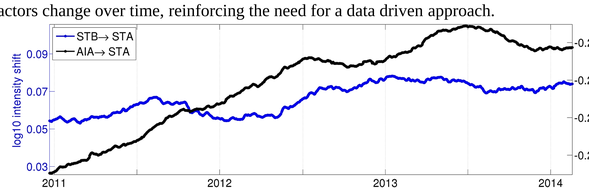

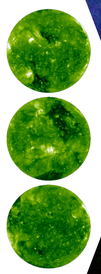

LIMB BRIGHTENING CORRECTION

MATLAB

DATA PRODUCT

Limb brightening effects can interfere with CH detection algorithms by increasing the intensity of CHs away from disk center. To try to equalize CH intensities, a limb-brightening correction curve (LBC) can be used. A theoretical LBC can be computed by using an idealized hydrostatic atmosphere approximation for a given coronal temperature as shown to the right.

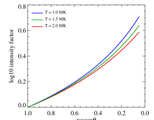

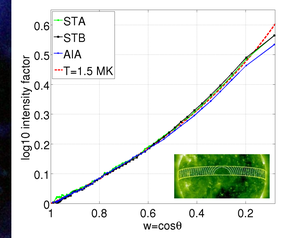

However, since the mean temperature changes over time and opacity effects can alter the curve, we again take a data-driven approach. We construct radially-dependent segments of the disk images and take average histograms over a one-year window in each radial bin. We then find the shift value required to align the central histogram with those of each radial bin. This is accomplished with the same left-side histogram SSE optimization used to compute the scale factors. In order to help maintain structure equivalence in the averaging radial segments, we limit the allowed latitude of the segments to a narrow band of +/- 0.1 radians from disk center (see left insert).

We have computed LBCs over the same time period and cadence as the scale factors. The LBC for 02/03/2011 is shown to the left as an example. We see that STA and STB closely match the theoretical curve of 1.5MK except near disk edge which may be explained by opacity effects. The noticeable separation of the AIA curve is not currently understood and may be due differences in the inherent optical and PSF properties of AIA vs EUVI and/or the thermal response curves of the EUVI/195 vs AIA/193 channels.